

Beyond Langevin Recombination: How Equilibrium Between Free Carriers and Charge Transfer States Determines the Open-Circuit Voltage of Organic Solar Cells

Timothy M. Burke, Sean Sweetnam, Koen Vandewal, and Michael D. McGehee*

Organic solar cells lag behind their inorganic counterparts in efficiency due largely to low open-circuit voltages (V_{oc}). In this work, a comprehensive framework for understanding and improving the open-circuit voltage of organic solar cells is developed based on equilibrium between charge transfer (CT) states and free carriers. It is first shown that the ubiquitous reduced Langevin recombination observed in organic solar cells implies equilibrium and then statistical mechanics is used to calculate the CT state population density at each voltage. This general result permits the quantitative assignment of V_{oc} losses to a combination of interfacial energetic disorder, non-negligible CT state binding energies, large degrees of mixing, and sub-ns recombination at the donor/acceptor interface. To quantify the impact of energetic disorder, a new temperature-dependent CT state absorption measurement is developed. By analyzing how the apparent CT energy varies with temperature, the interfacial disorder can be directly extracted. 63–104 meV of disorder is found in five systems, contributing 75–210 mV of V_{oc} loss. This work provides an intuitive explanation for why qV_{oc} is almost always 500–700 meV below the energy of the CT state and shows how the voltage can be improved.

to efficiently photogenerate charges.^[2,3] However, they have low open-circuit voltages and typically cannot be made optically thick while maintaining high fill factors.^[4,5] For comparison, the best silicon solar cell has a bandgap of 1.1 eV and an open-circuit voltage of 0.71 V, corresponding to a difference between the bandgap and qV_{oc} of only 0.40 eV.^[1] In contrast, one of the best performing organic solar cells, PTB7:PC₇₁BM, has an optical gap of 1.65 eV and an open-circuit voltage of 0.76 V, a difference of 0.89 eV.^[6] The lower qV_{oc} of organic solar cells relative to their optical gaps directly translates into lower power conversion efficiencies.^[7]

Some of this voltage loss is known to occur during the charge generation process when the initial photoexcitation produced by absorbing light is split at the heterointerface between donor and acceptor materials to form a charge transfer (CT) state, which is an interfacial electronic

state composed of an electron in the acceptor material and a nearby hole in the donor material that can directly recombine back to the ground state.^[8] In order to provide a driving force for this exciton splitting process to occur, donor and acceptor materials are typically chosen to have electron affinities that differ by 0.1–0.3 eV, which also reduces qV_{oc} by the same amount.^[9,10] Since the voltage loss between optical absorption and CT state formation is thought to be a necessary tradeoff in order to efficiently split excitons, V_{oc} is often referenced to the CT state energy rather than the optical gap.^[4,9–11] Even by this metric, however, the voltage is still quite low, with almost all organic solar cells having qV_{oc} between 0.5 and 0.7 eV below the CT state energy.^[4,12] In this work, we explain why the open-circuit voltage of organic solar cells has remained persistently low and develop a theory that provides guidance on how to improve it. Our key results and the relevant energy levels for understanding V_{oc} are summarized schematically in **Figure 1**.

1. Introduction

Organic solar cells (OPV) have the potential to become a low-cost technology for producing large-area, flexible solar modules that are ideal for tandem, portable, and building-integrated applications. However, they are not yet commercially competitive due to their low power conversion efficiencies ($\approx 10\%$) relative to those of silicon ($\approx 25\%$).^[1] Thus, a key challenge confronting the field of OPV is raising the power conversion efficiency (PCE). Since the PCE of a solar cell is the product of its short-circuit current (J_{sc}), open-circuit voltage (V_{oc}), and fill factor (FF), we can divide this task into three separate components.

High-performance organic solar cells have internal quantum efficiencies (IQEs) near 100% indicating that the devices are able

T. M. Burke, S. Sweetnam, Prof. M. D. McGehee
Stanford University Department of Materials Science
476 Lomita Mall, Stanford, CA 94022, USA
E-mail: mmcgehee@stanford.edu
Prof. K. Vandewal
Institut für Angewandte Photophysik
Technische Universität Dresden
01062 Dresden, Germany



DOI: 10.1002/aenm.201500123

2. Background Information

In order to understand V_{oc} , we will need to build a model that describes how electrons and holes recombine in organic solar cells and how this process depends on voltage. Since our goal is to develop an understanding of V_{oc} that will allow for the

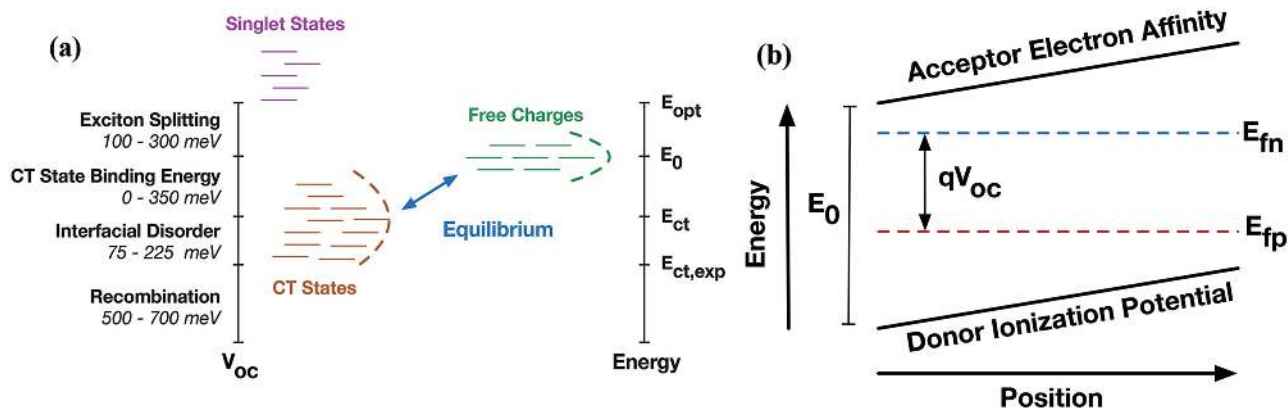


Figure 1. a) The sources of open-circuit voltage losses from the optical gap in an organic solar cell and various energy levels in the device to which they correspond. The specific losses for exciton splitting (electron transfer), the CT state binding energy, and free carrier recombination are based on previous literature reports. The loss due to interfacial disorder is presented in this work and the magnitude of the recombination loss is explained. b) Schematic band diagram of an organic solar cell at open-circuit, showing the relationship between the quasi-Fermi levels for electrons (E_{fn}) and holes (E_{fp}), E_0 , and the open-circuit voltage (V_{oc}).

rational design of organic solar cells with improved voltages, the theory must not only explain the available experimental data, but also provide useful insights that can guide the future design of materials. For example, would slightly raising the dielectric constant of organic semiconductors have a significant or marginal impact on V_{oc} ?^[13,14] Is there an open-circuit voltage tradeoff in using energy cascades to improve charge separation?^[15,16] Will raising the mobility of charge carriers in order to improve the fill factor also cause a decrease in open-circuit voltage by making carriers encounter each other more frequently?^[17] Finally, is V_{oc} low simply because of the large amounts of energetic disorder present in OPV materials?^[18] The theory we develop in this work will allow us to answer all of these questions.

It will be useful in our discussion to refer to two distinct but related quantities: E_{ct} and E_0 . E_{ct} is the average energy of all of the CT states in an organic solar cell and E_0 is the average difference between the electron affinity (EA) of the acceptor material and the ionization potential (IP) of the donor at the interface between the two. Since organic solar cells are disordered, there is not one single value for either the CT state energy or the EA–IP difference; instead, we have to work with average quantities. We specify that E_0 should be averaged only over the interfacial/mixed portions of the device since both the EA and IP are known to be different in aggregated versus mixed regions of many organic solar cells and we wish to compare E_0 with the energy of a CT state that only forms at an interface.^[15,19] If there were no interaction between the electron and hole in the CT state, E_{ct} would equal E_0 . In general, they are related by

$$E_{ct} = E_0 - E_B, \quad (1.1)$$

where E_B is the average CT state binding energy.^[8,14] We can estimate E_B based on the dielectric constant of organic semiconductors and the average separation between the electron and hole in the CT state (r_{ct}) using Coulomb's law

$$E_B = \frac{q^2}{4\pi\epsilon r_{ct}}, \quad (1.2)$$

where q is the charge of an electron and ϵ is the dielectric constant of the material. Experiments have estimated average CT state separations between 1 and 4 nm and organic semiconductors typically have relative dielectric constants between 3 and 5 so we would expect values for E_B between 70 and 480 meV.^[14,20,21] Recently, Chen et al. developed a technique to measure E_B and reported values between 0 and 350 meV for seven different polymer–fullerene systems, which compares well with our simple calculation.^[14]

The reason we emphasize the distinction between E_{ct} and E_0 is because a large body of work has established that in optimized organic solar cells recombination is a two-step process. The electron and hole first meet at the interface between the donor and acceptor materials and form a CT state, which then either recombines or dissociates back into free carriers.^[22–25] We will find that we can determine whether recombination is limited by the rate at which free carriers form CT states or the rate at which those CT states recombine by analyzing if V_{oc} correlates more strongly with E_0 or E_{ct} . So it is important to establish that the two numbers are distinct and that the difference can be measured experimentally.^[11,14]

In either case, since recombination involves one electron and one hole, the law of mass action states that its rate is proportional to the product of the electron and hole concentrations (n and p , respectively)

$$R = knp, \quad (1.3)$$

where R is the rate of recombination per unit volume and k is a proportionality constant. Under open circuit conditions, where the quasi-Fermi levels are flat, we can directly relate the product np (though not the individual concentrations n or p) to the voltage of the solar cell (see Figure 1 for variable definitions)

$$np = N_0 \exp\left(\frac{E_{fn} - E_{fc}}{kT}\right) * N_0 \exp\left(\frac{E_v - E_{fp}}{kT}\right), \quad (1.4)$$

$$np = N_0^2 \exp\left(\frac{qV_{oc} - E_0}{kT}\right),$$

where N_0 is the density of electronic states in the device, typically taken to be around 10^{21} cm^{-3} (1 nm^{-3}) for organic semiconductors, E_c is the acceptor electron affinity, and E_v is the donor ionization potential.^[26,27] The built-in potential of the solar cell and the possible presence of band-bending do not affect this result since they change E_c and E_v in the same manner, canceling out in the expression for np .

In general, k must be measured experimentally, however, in certain limiting cases an analytical expression can be found. One such case is Langevin recombination, where every time an electron and hole meet, they recombine.^[22,28] In this limit, the recombination rate constant has been shown to be

$$k_{\text{lan}} = \frac{q(\mu_e + \mu_h)}{\epsilon}, \quad (1.5)$$

where μ_e is the electron mobility and μ_h is the hole mobility. Langevin recombination has been experimentally validated for organic light emitting diodes (OLEDs) and is often also applied to OPV.^[22,29–33] However, for organic solar cells it overpredicts the measured recombination rates by a material system and temperature-dependent factor as high as 10^4 for P3HT:PCBM though typically between 10 and 100.^[22,33,34] Device modelers account for this discrepancy by introducing a “Langevin reduction factor” that artificially lowers k_{lan} until it agrees with experiment.^[22]

In the absence of a better alternative, most researchers have described recombination in organic solar cells in terms of reduced Langevin recombination.^[22,33,34] However, the theory has not been able to provide useful guidance on how to improve V_{oc} . For example, based on Equation (1.5) we would expect that raising the charge carrier mobilities would reduce V_{oc} by making free carriers recombine quicker. It is difficult to test this prediction experimentally since we do not have precise control over the charge carrier mobilities but it is typically observed that organic solar cell efficiencies actually improve with higher mobilities because the fill factor increases without a corresponding loss in open-circuit voltage.^[5,35] Langevin theory would also imply that slight changes in dielectric constant should have a negligible effect on V_{oc} . Recalling that the open-circuit voltage of any solar cell depends logarithmically on the recombination rate, Equation (1.5) says that changing the dielectric constant from 3 to 5 should only improve the open-circuit voltage by^[22]

$$\Delta V_{\text{oc}} = \frac{kT}{q} \ln\left(\frac{5}{3}\right) \approx 0.013 \text{ V}. \quad (1.6)$$

This would mean that the OPV community should not look to slight dielectric constant increases as a meaningful way to improve V_{oc} . In contrast, Chen et al. recently showed that changing ϵ_r from 3 to 5 modified the measured open-circuit voltage by hundreds of mV and that the dependence of V_{oc} on ϵ_r was approximately linear.^[14] A linear dependence of V_{oc} on ϵ_r means that recombination must actually depend exponentially on the dielectric constant. Several other authors have also altered the dielectric constant of an organic solar cell by methods such as modifying the polymer sidechains or adding a high-dielectric-constant additive. All of these studies found large (>100 mV) open-circuit voltage gains for slight dielectric

constant improvements, which is inconsistent with a logarithmic dependence of V_{oc} on ϵ_r .^[36,37]

3. The Temperature Dependence of V_{oc} Leads Us Beyond Langevin Theory

Before presenting our model, we would like to review what is known about the temperature dependence of V_{oc} because it strongly hints at what needs to be added to complete the theory. Looking at Equation (1.4), we can see that Langevin recombination predicts that V_{oc} should depend on E_0 . Equating the recombination current with the short-circuit current to solve for V_{oc} gives

$$qV_{\text{oc}} = E_0 - kT \log\left(\frac{qN_0^2 L k_{\text{lan}}}{J_{\text{sc}}}\right), \quad (1.7)$$

where L is the thickness of the device and J_{sc} is its short-circuit current.

Equation (1.7) implies that looking across material systems we should see strong correlations between V_{oc} and E_0 in each system. In fact, while V_{oc} does tend to increase with E_0 , the trends in open-circuit voltage across a large number of material systems are best described by changes in CT state energy, not by changes in E_0 .^[4,12,14,38] Given that V_{oc} has been shown to be linearly related to E_{ct} across many systems with deviations less than 200 meV and that the difference between E_{ct} and E_0 varies by more than 300 meV, it would be very difficult to explain the observed dependence of V_{oc} on E_{ct} if it actually depended on E_0 instead.^[4,14] Another consequence of this dependence is that if we cool an organic solar cell down to cryogenic temperatures, Langevin theory predicts that V_{oc} will approach E_0 (details in the Supporting Information). In fact, when extrapolated to 0 K, V_{oc} does not approach E_0 but instead converges to the CT state energy.^[11,14,39] Since the temperature-dependent experiments are performed on a single solar cell and not by comparing different material systems, there is no scatter in the data and the discrepancy is very clear.

Intuitively, if every time free carriers meet they recombine, there is no way for the value of E_{ct} to affect their behavior since by the time the carriers are close enough to experience E_{ct} their fate is already determined. On the other hand, if the carriers were able to form CT states several times and split before finally recombining then an equilibrium could exist between CT states and free carriers, in which case E_{ct} would be critically important because the density of CT states would be proportional to a Boltzmann factor involving E_{ct} . This raises the question of whether Langevin theory mispredicts the recombination rate in organic solar cells because it overestimates the frequency with which free carriers meet each other or because only a small fraction of those encounters lead to recombination. Several authors have explored this issue and shown with kinetic Monte Carlo simulations that k_{lan} actually does a surprisingly good job of predicting how often carriers encounter each other, even in disordered material systems, which agrees with the fact that the expression works reasonably well for OLEDs.^[31,32] This implies that the Langevin reduction factor must be necessary because not every encounter between free carriers results

in recombination. Recent experimental work has confirmed this hypothesis by showing that the low energy CT states that would be formed by free carriers encountering each other have the same high splitting efficiency as higher energy CT states formed during the photogeneration process.^[40] The CT state splitting process has also been investigated using detailed kinetic Monte Carlo simulations, which show that carriers actually have a very low chance of recombining during any given encounter.^[16,41–44] The likely reason that Langevin recombination works for OLEDs is because those systems have been specifically designed for free carriers to efficiently find each other and recombine. Organic solar cells, on the other hand, have been specifically designed to prevent this process.

4. Reduced Langevin Recombination Implies Equilibrium

The suggestion that most charge transfer states recombine has been made before as an explanation for the Langevin reduction factor and detailed numerical models have been constructed to explore its impact.^[32,45] For example, Hilczner and Tachiya were able to accurately reproduce the temperature dependence of the Langevin reduction factor with a model that allowed CT states to split back into free carriers.^[45] In this work, we would like to take the idea one step further. If free carriers form CT states and split much faster than they recombine, there should be time for equilibrium to be reached between the population of free carriers and the population of interfacial CT states. In this limit, it does not matter how quickly carriers move, a certain fraction of them will always be in CT states and that fraction can be calculated using Boltzmann statistics and a knowledge of the free energy difference between free carrier states and charge transfer states. In order to see if such a description is appropriate, however, we must first investigate how close to equilibrium the free carrier and CT state populations are in an organic solar cell. When carriers meet and split 10 000 times before recombining, there is clearly time for equilibrium to be established between the two populations; however, it is not obvious that the same is true when they only meet and split ten times.

We can answer this question using a kinetic model. **Figure 2** shows the recombination process schematically with all of the relevant rates labeled. Without making any assumptions about whether free carriers and CT states are in equilibrium with

each other, we can write down rate equations describing the interactions between the two populations

$$\begin{aligned} \frac{dn_{ct}}{dt} &= k_m np - (k_r + k_s) n_{ct}, \\ \frac{dn}{dt} &= -k_m np + k_s n_{ct} + G, \\ \frac{dp}{dt} &= -k_m np + k_s n_{ct} + G, \end{aligned} \quad (1.8)$$

where n_{ct} is the density of CT states, k_r is the (average) rate constant at which CT states recombine, k_s is the rate constant at which CT states split back into free carriers, k_m is the rate constant at which free carriers meet, and G is the rate at which free carriers are being generated. Since the solar cell is in steady state, we know that n and p are being replenished, either by injected carriers from the contacts or by photogenerated carriers, at precisely the same rate that the CT states are recombining so $G = k_r n_{ct}$. Solving for steady state leads to

$$\frac{n_{ct}}{np} = \frac{k_m}{k_r + k_s}. \quad (1.9)$$

We can also define the equilibrium density of CT states (n_{ct}^{eq}) we would expect if k_r were much slower than k_s as

$$\frac{n_{ct}^{eq}}{np} = \frac{k_m}{k_s}. \quad (1.10)$$

Since we argued before that the Langevin reduction factor (γ) primarily measures the fraction of free carrier encounters that lead to recombination, we can use it to relate k_r and k_s

$$\gamma = \frac{k_r}{k_r + k_s}, \quad (1.11)$$

$$k_r = \frac{\gamma}{1 - \gamma} k_s. \quad (1.12)$$

If the rate of CT state recombination is much faster than CT states splitting back into free carriers, then γ approaches 1 and Langevin theory applies. In the other limit, γ approaches 0 and equilibrium holds between free carriers and CT states. To quantify how close to equilibrium free carriers and CT states are,

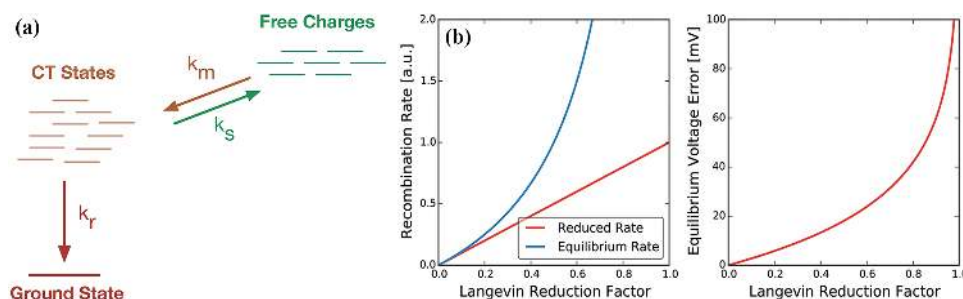


Figure 2. a) Kinetic scheme describing the recombination process in organic solar cells. b) The difference in recombination rate and predicted V_{oc} between the reduced Langevin recombination expression and the equilibrium approximation as a function of the Langevin reduction factor.

we can compare the recombination rate that we would expect at equilibrium (R_{eq}) with the reduced Langevin recombination expression (R_{lan})

$$\begin{aligned} R_{\text{lan}} &= \gamma k_m np, \\ R_{\text{eq}} &= k_r n_{\text{ct}}^{\text{eq}} = \frac{\gamma}{1-\gamma} k_m np. \end{aligned} \quad (1.13)$$

Figure 2 plots both recombination expressions as a function of γ . The goal is to determine how small γ needs to be before an equilibrium description becomes appropriate. We find that once the Langevin reduction factor is smaller than about 0.1, the reduced Langevin recombination rate is extremely close to the rate expected if the free carriers were fully in equilibrium with charge transfer states. Furthermore, since V_{oc} depends on recombination in a logarithmic fashion, even a solar cell with a Langevin reduction factor of 0.5 would have an open circuit voltage that deviates from the equilibrium prediction by less than 20 mV and in fact γ must be very close to 1 before the equilibrium picture breaks down. Almost all organic solar cell materials have $\gamma \leq 0.2$, so we can treat bimolecular recombination as occurring from a population of free carriers in equilibrium with CT states (tabulated reduction factors and more discussion of this point is presented in the Supporting Information).^[33] This means that we do not need a complicated numerical model to estimate k_s and calculate γ in order to understand the open-circuit voltage of organic solar cells; we can instead just write down the density of CT states based on the requirement that they be in equilibrium with free carriers.

5. Equilibrium Simplifies the Understanding of V_{oc}

When chemical or electronic species are in equilibrium with each other the fundamental requirement is that there must not be a thermodynamic driving force to convert one species into another. In the case of CT states, it means that the free energy gained by creating one additional CT state must be exactly equal to the free energy lost by destroying a free electron and free hole, otherwise nature could lower its free energy by simply converting one more electron/hole pair into a CT state or vice versa and this reaction would spontaneously happen. This is a very general condition for equilibrium that holds both for electrons and holes as well as for atoms and molecules. It underlies the law of mass action and the calculation of equilibrium constants for chemical reactions. In chemistry, the free energy of a species is often called its chemical potential. In solid-state physics, the free energy of an electron is called its quasi-Fermi level. By convention, however, the quasi-Fermi level of holes is defined to have the opposite sign as its free energy, which is why holes “float” in semiconductor band diagrams. In short, equilibrium between electronic species allows us to relate their quasi-Fermi levels since this is the quantity that measures their molar free energies and at equilibrium it is their free energy that must be equal, not, for example, their concentrations.

So, equilibrium between CT states and free carriers requires that the chemical potential of the CT states (μ_{ct}) be equal to the difference of the electron and hole quasi-Fermi levels for their molar free energies to be equal

$$\mu_{\text{ct}} = E_{\text{fn}} - E_{\text{fp}}. \quad (1.14)$$

For further discussion of the relationship between quasi-Fermi levels and chemical potentials, readers are directed to a lengthy treatment by Wurfel, who validated and used the same approach to relate the quasi-Fermi levels of electrons and holes with the chemical potential of photons in order to derive the semiconductor electroluminescence spectrum.^[46] For readers who prefer an alternative derivation that does not require introducing chemical potentials, we arrive at the same result in the Supporting Information directly from the canonical ensemble in statistical mechanics by considering the many-particle partition function of electron–hole pairs in an organic solar cell.

We specified the chemical potential of the CT state population using Equation (1.14) because we know that at open-circuit the difference between the electron and hole quasi-Fermi levels is constant across the device and given by qV_{oc}

$$E_{\text{fn}} - E_{\text{fp}} = qV_{\text{oc}} = \mu_{\text{ct}}. \quad (1.15)$$

Equation (1.15) means that equilibrium between free carriers and CT states gives us a way to directly relate the open-circuit voltage to the chemical potential of the CT states, letting us calculate the number of CT states without needing to know how many free carriers there are in the device, how quickly they are moving or what the energetic landscape for those free carriers looks like.

Now that we know the chemical potential of the CT states, we can determine how many are occupied (N_{ct}) by integrating over the density of possible CT states, $g_{\text{ct}}(E)$ (see **Figure 3**). Intuitively, one can think of μ_{ct} as measuring the amount of free energy the system can use to populate CT states. It makes sense then that by combining this information with knowledge of how much energy it takes to occupy each CT state and how many possible CT states there are, i.e., the density of states, you can calculate the total number of populated states. For readers familiar with the standard expressions relating electron and hole quasi-Fermi levels to electron and hole densities, the result for CT states is exactly analogous. The precise functional form for all three expressions is typically derived from the grand canonical ensemble in statistical mechanics and worked out step by step for the case of CT states in the Supporting Information. Here, we quote the result

$$N_{\text{ct}} = \int_{-\infty}^{\infty} g_{\text{ct}}(E) \exp\left(\frac{\mu_{\text{ct}} - E}{kT}\right) dE. \quad (1.16)$$

As a first approximation, we show in the Supporting Information that the CT state distribution should have a Gaussian shape, as is typical for inhomogeneously broadened energy levels, which means this integral can be computed analytically (see references and calculation in the Supporting Information).^[18,47–49] If the standard deviation of the CT state distribution is σ_{ct} and its center is E_{ct} , then

$$N_{\text{ct}} = fN_0 \exp\left(\frac{\sigma_{\text{ct}}^2}{2(kT)^2}\right) \exp\left(\frac{qV_{\text{oc}} - E_{\text{ct}}}{kT}\right), \quad (1.17)$$

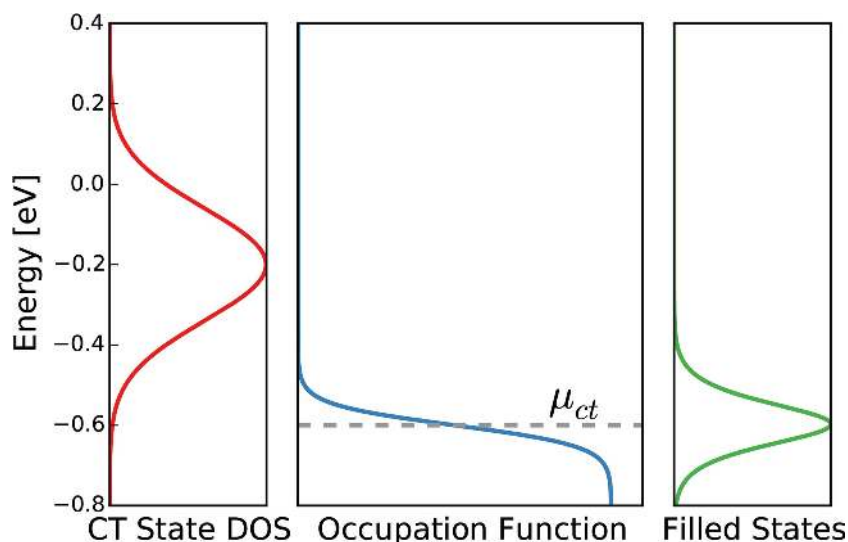


Figure 3. Schematic showing how the density of available CT states, $g_{ct}(E)$, combined with knowledge of the CT state chemical potential, μ_{ct} , permits the calculation of the number of filled CT states, N_{ct} .

where f is the volume fraction of the solar cell that is mixed or interfacial. Each of these CT states recombines with an average lifetime $\tau_{ct} = 1/k_r$, so the recombination current in the solar cell can be written as

$$J_{rec} = \frac{qN_{ct}L}{\tau_{ct}} = \frac{qfN_0L}{\tau_{ct}} \exp\left(\frac{\sigma_{ct}^2}{2(kT)^2}\right) \exp\left(\frac{qV_{oc} - E_{ct}}{kT}\right), \quad (1.18)$$

where L is the thickness of the solar cell. Now that we have an expression for recombination as a function of V_{oc} , we can invert it and solve for V_{oc} since at open-circuit $J_{rec} = J_{sc}$

$$qV_{oc} = E_{ct} - \frac{\sigma_{ct}^2}{2kT} - kT \log\left(\frac{qfN_0L}{\tau_{ct}J_{sc}}\right). \quad (1.19)$$

Similar expressions relating V_{oc} and E_{ct} but excluding the effects of disorder have been derived previously by various methods including detailed balance relationships and solar cell equilibrium with a black body.^[39,50–52] The benefit of our approach is that by explicitly considering an illuminated organic solar cell with interfacial disorder and an arbitrary energetic landscape for free carriers we remove any ambiguity about when the result is applicable, show how it is equivalent to reduced Langevin recombination and connect all of the input parameters directly with concrete material properties that can either be measured or calculated. This last point is critical as it will allow us to explain why qV_{oc} is so consistently 0.5–0.7 eV below the measured CT state energy in almost all organic solar cells, despite the widely varying electronic properties among those different systems.

Our result shows that, in the absence of device imperfections like contact pinning or shunts, V_{oc} is determined solely by the degree of mixing in the device, the energy of the center of the CT state distribution, the degree of energetic disorder in the mixed region, and the CT state lifetime. The CT state

lifetime describes the rate at which CT states directly recombine either radiatively or non-radiatively. It is distinct from the free carrier lifetime that could be measured in a transient photovoltage experiment as we discuss below.

6. Effects of an Energy Cascade in Three-Phase Bulk Heterojunctions

One of the reasons we derived our expression for V_{oc} in terms of quasi-Fermi levels instead of free carrier densities is because it makes it clear that there is no dependence of V_{oc} on the energy levels of free carriers, i.e., E_0 appears nowhere in our expression for V_{oc} and we did not need to make any assumptions about the energetic landscape for free carriers in order to derive it. This is not to say that the energetic landscape is unimportant for solar cell operation, just that our theory shows it does not affect the numerical value of the open-circuit voltage. When calculating the potential efficiency of a solar cell material, one is typically not interested in V_{oc} in isolation but in the difference between the optical gap and qV_{oc} since a device with a smaller optical gap absorbs more light and can compensate for its lower voltage with additional photocurrent, increasing the overall efficiency. To use an extreme example, silicon solar cells have lower open-circuit voltages than many OPV devices, but this does not mean that organic solar cells are more efficient. So, if one is able to decrease the optical gap of an organic solar cell without affecting the CT state energy, then, our theory says that within certain limits discussed below, the photocurrent should increase without a corresponding decrease in the open-circuit voltage. A potential way to achieve this would be by introducing controlled energy cascades.

To explore what happens at open-circuit in a three-phase bulk-heterojunction with an energy cascade, let us consider two example situations as shown in **Figure 4**. In one case, we have an organic solar cell that is one-third mixed, one-third aggregated acceptor, and one-third aggregated donor but has uniform energy levels for free carriers in all of the phases. In the other case, we have an energy cascade where the mixed region is identical to the first case but the aggregated regions have energy levels that are shifted by 100 meV each. In both cases, we will consider $E_0 = 1.7$ eV, $E_{ct} = 1.5$ eV, $N_0 = 10^{21}$ cm⁻³, and 80 meV of Gaussian disorder in each of the energy levels. For clarity we will ignore the built-in potential so that the carrier densities are constant in each phase and calculated using Equation (1.4). The presence of a built-in potential does not change our conclusion it just makes the calculation less intuitive. We want to determine the density of free carriers and CT states as well as the recombination rate and free carrier lifetime at an open-circuit voltage of 0.9 V.

Without the energy cascade, we calculate the average free electron and hole densities to be 1.6×10^{16} cm⁻³ and the density of CT states to be 3.6×10^{12} cm⁻³. In a 100-nm-thick device with a CT state lifetime of 500 ps, this would correspond to a

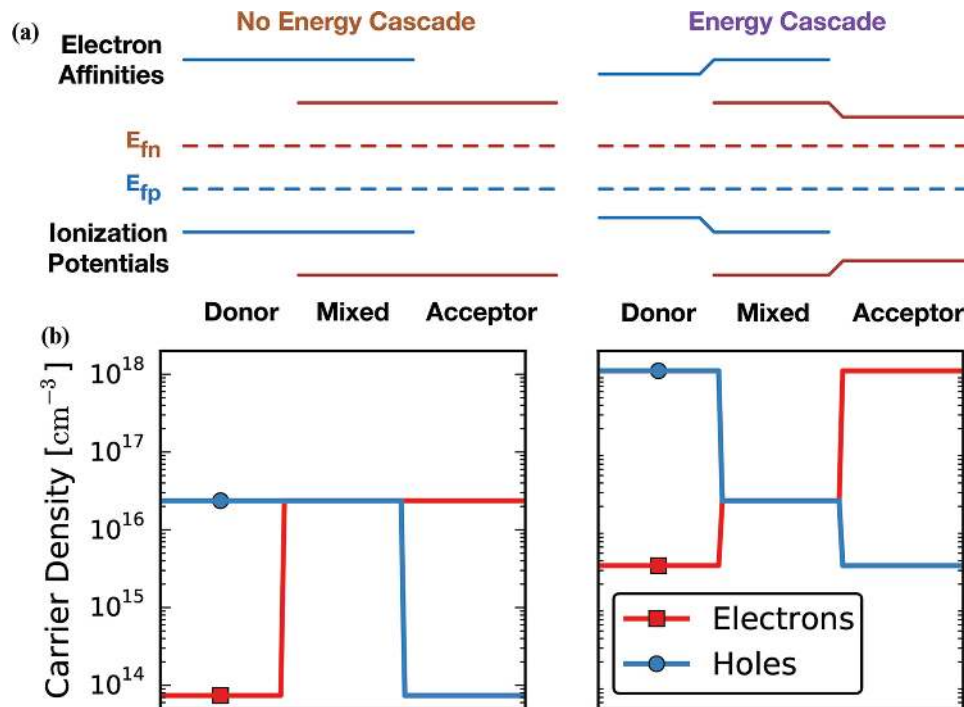


Figure 4. Two example energy diagrams showing a solar cell with and without an energy cascade between mixed and aggregated phases. The bottom plots show the carrier density in each phase assuming a IP–IP and EA–EA offset between the donor and acceptor materials of 150 meV each.

recombination current of 12 mA cm^{-2} . Even though the CT state lifetime is only 500 ps, there are 4390 times more free carriers than CT states, so each carrier, on average, has only a 1 in 4390 chance of occupying a CT state. Since transient photovoltage measures the lifetime of the average carrier, one would measure a free carrier lifetime of

$$500 \text{ ps} * 4390 = 2.2 \mu\text{s}. \quad (1.20)$$

With the energy cascade, the density of CT states and free carriers in the mixed region is unchanged since E_{ct} and E_0 are unchanged but there are now many more free carriers in the aggregated regions so that the average density of carriers has increased to $4 \times 10^{17} \text{ cm}^{-3}$. The recombination current is the same since both the number of CT states and their lifetimes are the same, which means the free carrier lifetime must have increased substantially to $53 \mu\text{s}$ since the odds of each free carrier occupying a CT state has decreased to 1 in $\approx 105\,000$.

If we only had access to information on the free carrier densities and lifetimes, for example, through charge extraction and transient photovoltage measurements, we would conclude that the solar cell with the energy cascade had substantially reduced recombination since both the free carrier lifetime and the density of free carriers at open-circuit increased significantly.^[53,54] However, the actual amount of recombination is the same in the two solar cells and the presence of the energy cascade neither increased nor decreased V_{oc} . This is one of the consequences of equilibrium between free carriers and CT states and it also implies that traps and energetic disorder outside of the mixed region, which would have a similar effect to an energy cascade, do not impact the open-circuit voltage. Put another

way, we are saying that for a given solar cell E_{ct} and E_0 will be related to each other because both involve the EA–IP difference. However, if one keeps E_{ct} constant but varies E_0 (using an energy cascade, for example), V_{oc} will not change. On the other hand, if one keeps E_0 constant but varies E_{ct} (by modifying the CT state binding energy, for example), V_{oc} will change to track the variation in E_{ct} . So, the important variable that determines V_{oc} is E_{ct} , not E_0 . If one changes E_0 and in-so-doing also changes E_{ct} (by changing the donor's IP, for example), then V_{oc} will, of course, also change. However, it changes because of the change in E_{ct} , not the change in E_0 .

We can use this effect to our advantage by introducing energy cascades that broaden the optical absorption without affecting the CT state energy to increase the photocurrent without sacrificing voltage.^[15] For example, both of the solar cells that we discussed above have the same open-circuit voltage but the one with the energy cascade could achieve this voltage with a 200 meV smaller optical gap, increasing the short-circuit current. This extra current comes at the expense of a reduced EA–EA offset between aggregated donor/acceptor phases, but provided the offset remains large enough to drive exciton splitting, there should be no impact on charge generation and energy cascades could be used as a way to recover some of the voltage lost due to overly large EA–EA offsets.

7. The Role of Energetic Disorder

Looking at Equation (1.19) and noting that the energetic disorder could easily be 100 meV, our model implies that we should expect significant variations in the difference between V_{oc} and

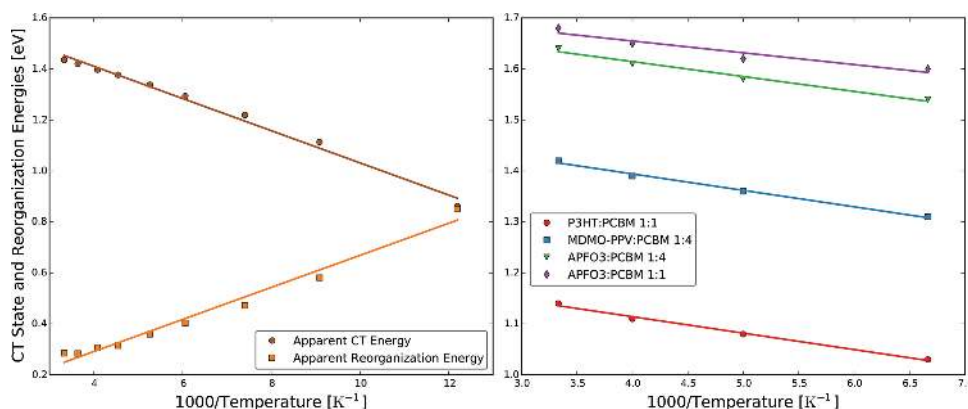


Figure 5. Fits to the temperature dependence of E_{ct}^{exp} for MDMO-PPV:PCBM, P3HT:PCBM, and AFPO3:PCBM (1:1 and 1:4 blend ratios). (Left) The extracted E_{ct} and reorganization energies for a blend of regiorandom P3HT:PCBM showing that they are both linear in $1/T$ and have very similar slopes (104.3 meV disorder is extracted from the slope of the CT state energy and 104.1 meV for the reorganization energy, fit independently). (Right) The temperature-dependent E_{ct} measurements taken from literature.^[11] The data points are the experimental fit parameters at each temperature and the lines are $1/T$ fits to the data.

E_{ct} based on differences in the amount of interfacial energetic disorder, which, in contrast to free carrier disorder, is predicted to affect the open-circuit voltage by setting the width of the CT state distribution. This would seem to be in contradiction to the experimental finding that qV_{oc} is almost always 0.5–0.7 eV below the CT state energy so we need to briefly discuss the relation between what we call E_{ct} and what is measured experimentally. Experimental values for E_{ct} are typically extracted by sensitively measuring the optical absorption of an organic solar cell below its optical gap.^[11,55,56] CT states weakly absorb light so they appear as a low-energy shoulder in the absorption spectrum of organic solar cell blends. Since the absorption of the CT states is vibrationally broadened, one cannot directly infer the energy of a CT state from the energy of the light that it absorbs. Instead, Marcus theory is used to calculate the energy of the state based on its absorption spectrum. Marcus theory describes the vibrational broadening of a single absorber in terms of its reorganization energy, λ , and has been very successful in fitting the CT state absorption spectrum in many OPV material systems.^[11,40,57] This is somewhat surprising since we do not expect to have a single CT state in organic solar cells but rather an inhomogeneously broadened distribution of CT states as described earlier. Thus, the absorption of the CT states is better described by the Marcus theory absorption expression for a single CT state integrated over the distribution of states. When the distribution is Gaussian in shape, the

resulting inhomogeneously broadened absorption turns out to be identical to that of a single Marcus theory absorber with an effective energy E_{ct}^{exp} and reorganization energy λ^{exp} given by (derivation in the Supporting Information)

$$E_{ct}^{exp} = E_{ct} - \frac{\sigma_{ct}^2}{2kT},$$

$$\lambda^{exp} = \lambda + \frac{\sigma_{ct}^2}{2kT}. \quad (1.21)$$

This result explains why it is possible to successfully fit the CT state absorption as if it were a single state, but it also means that the experimentally measured CT state energy already incorporates the presence of energetic disorder. In Figure 5a, we verify this prediction by measuring the CT state absorption of a 1:4 Regiorandom P3HT:PCBM blend as a function of temperature using Fourier transform photocurrent spectroscopy (FTPS).^[55] We find that both E_{ct}^{exp} and λ^{exp} are linear in $1/T$ with opposite slopes that are very similar in magnitude, consistent with our theoretical prediction. Fits to the data yield values for σ_{ct} of 104.3 and 104.1 meV from the CT state and reorganization energies, respectively.

In Figure 5b, we use this new tool to extract the interfacial energetic disorder from previously published temperature-dependent measurements of E_{ct}^{exp} .^[11] We find σ_{ct} for MDMO-PPV, P3HT, and AFPO3 blended with PCBM to be between 60 and 75 meV. The results are summarized in Table 1.

Table 1. Extracted CT state distribution centers and standard deviations with experimental V_{oc} measurements for comparison. All raw data except for RRa P3HT are from literature.^[11]

Material system	E_{ct} [eV]	σ_{ct} [meV]	E_{ct}^{exp} [eV]	V_{oc} [V]	$E_{ct} - qV_{oc}$ [eV]	$E_{ct}^{exp} - qV_{oc}$ [eV]
P3HT:PCBM 1:1	1.24	75	1.14	0.61	0.61	0.53
RRa P3HT:PCBM 1:4	1.66	104	1.44	0.83	0.83	0.61
MDMO-PPV:PCBM 1:4	1.52	75	1.42	0.84	0.68	0.58
APFO3:PCBM 1:4	1.73	71	1.64	1.05	0.68	0.59
APFO3:PCBM 1:1	1.74	63	1.68	1.09	0.65	0.59

Using Equation (1.21) we can now simplify our expression for V_{oc} to

$$qV_{oc} = E_{ct}^{exp} - kT \log \left(\frac{qfN_0L}{\tau_{ct}J_{sc}} \right) \quad (1.22)$$

and see that the dependence of V_{oc} on interfacial disorder is exactly masked by the experimental techniques used to measure E_{ct} .

8. Experimental Observations Explained by the Model

Our model predicts that V_{oc} should increase linearly as we lower the temperature of the solar cell and appear to converge to E_{ct}^{exp} when extrapolated to 0 K as seen experimentally and in contrast to the predictions of Langevin recombination. It also explains why $E_{ct}^{exp} - qV_{oc} \approx 0.6$ eV for many systems that have been studied even though they had different amounts of energetic disorder since only interfacial energetic disorder matters and the available techniques to measure E_{ct} happen to be affected by interfacial disorder in precisely the same way as V_{oc} . We see why V_{oc} is exponentially dependent on the dielectric constant, since that sets the CT state binding energy, which determines, at equilibrium, what fraction of free carriers will be in a CT state via a Boltzmann factor. We also see why the highly variable energetic landscape for free carriers, including ubiquitous energy cascades between aggregated and mixed regions, does not impact the difference between E_{ct}^{exp} and V_{oc} since the number of populated CT states at equilibrium depends only on the CT state energy and the open-circuit voltage.^[15] Finally, we see that the carrier mobility does not affect V_{oc} because the recombination process is not limited by the rate at which free carriers find each other.

9. Explaining the Magnitude of the Voltage Loss

We now turn to the empirical result that qV_{oc} is almost always 0.5–0.7 eV below E_{ct}^{exp} .^[4] To compare our model with experiment we need to estimate the expected ranges of all of the necessary input parameters. We start with the volume fraction of interfaces and mixed regions in organic solar cells. On the high side, we have solar cells like regiorandom P3HT that are completely amorphous, so the solar cell could be 100% mixed. On the low side we have low-donor-content cells (1%–10% mixed) and bilayers. Even a perfect 100 nm bilayer would still be $\approx 1\%$ interface (1 nm of donor/acceptor molecules involved in an interface in a 100 nm thick active layer), so we conclude that organic solar cells are between 1% and 100% mixed.

We also need to know the CT state recombination lifetime. This quantity is difficult to measure experimentally since the distribution of CT states excited in the transient experiments used to measure CT state recombination rates is far from equilibrium, meaning that the average lifetime of those CT states may differ from that of the equilibrium distribution that exists at steady state. We discuss this point at more length in the Supporting Information and present tabulated lifetimes from

literature. In this section, we summarize the available estimates of τ_{ct} from a variety of experimental and theoretical methods. Ultrafast pump–push measurements and photoluminescence studies tend to report lifetimes between 100 ps and several ns.^[58–60] Quantum chemical calculations on a P3HT:PCBM analog predict 500 ps for one model and as fast as 90 ps for a different interface conformation.^[61,62] Further calculations have shown that the donor/acceptor interface is actually dynamic on the timescale of 10 ns so even if a particular interfacial conformation would lead to very slow recombination, the interface will explore enough conformations within 10 ns to find one that allows for fast recombination.^[62] Given the experimental and computational variability, we consider a range of lifetimes between 10 ps and 10 ns, keeping in mind that at the low end of the lifetime range we do not necessarily expect there to be time for complete equilibrium to develop between free carriers and CT states. However, as we showed in Figure 2, we do not actually need full equilibrium for the predictions of our theory to be accurate; we simply need τ_{ct} to be non-negligible such that CT states dissociate several times before recombining, which we generally know to be the case since the solar cells were able to photogenerate free carriers in the first place.^[40]

In principle, we also need to know the degeneracy of the charge transfer states. It is tempting to assume that there is one CT state for each pair of nearest neighbor donor/acceptor molecules, however, a range of experimental and theoretical work has shown that CT states form between non-nearest neighbor molecules as well due to long-range couplings between non-adjacent molecules.^[21,63–65] This effect is shown in Figure 6a and is very important because if you consider only CT states forming between molecules 1 nm apart, you might expect three CT states per acceptor molecule since three of its six nearest neighbors in a simple cubic, 50:50 blend of donor or acceptor molecules would be donors. On the other hand, if you increase the interaction distance to 2 nm, you would have 33 molecules with which each acceptor can interact and ≈ 16 CT states. At 3 nm it would be 113 molecules and 56 CT states per acceptor. In general, the density of CT states increases like the cube of the CT state delocalization length. Previous authors have discussed the importance of CT state delocalization for improving charge generation.^[21] Here, we add that increased delocalization is also likely to limit the open-circuit voltage by providing more pathways through which recombination can occur, implying a design tradeoff that will need to be optimized. We find good agreement with experimental V_{oc} measurements at 32 CT states per acceptor molecule (an approximate delocalization length of 2.5 nm). Answering the question of precisely how many CT states are formed at each interface would be an important candidate for future quantum chemical calculations.

Figure 6b explores the expected difference between V_{oc} and E_{ct}^{exp} for a 100-nm-thick active layer with a short-circuit current of 10 mA cm⁻² across the range of plausible material parameters that we found in the preceding paragraphs.

The key point to take away from Figure 6b is that almost all combinations of material parameters will result in an open-circuit voltage between 0.5 and 0.7 V below E_{ct}^{exp} , explaining why this empirical rule has worked so well. This is a consequence, however, of the range of CT state lifetimes and degrees of mixing observed in organic solar cells. More precisely, we

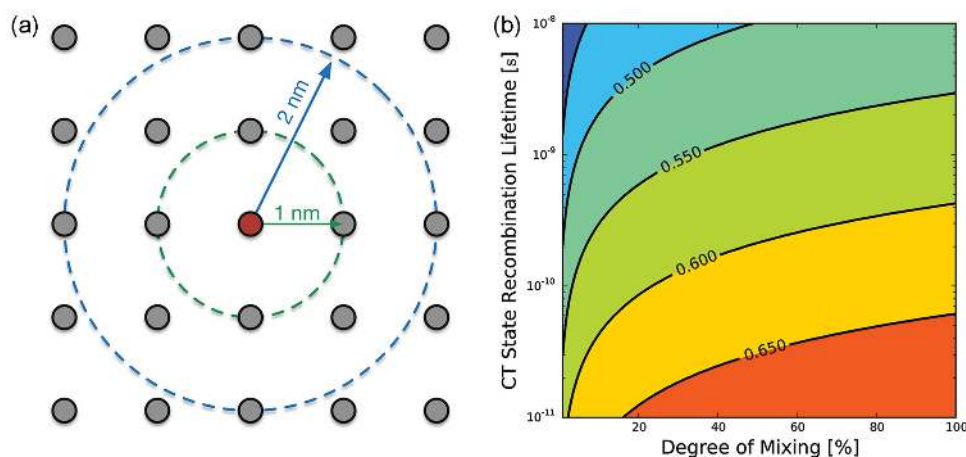


Figure 6. a) A 2D schematic showing the effect of CT state delocalization on the number of CT states in an organic solar cell. Gray circles indicate molecules and dashed lines show different delocalization lengths. b) The expected voltage difference (V) between E_{ct}^{exp}/q and V_{oc} for a 100 nm thick active layer with a J_{sc} of 10 mA cm^{-2} . A constant molecular density of 10^{21} cm^{-3} [1 nm^{-3}] is used with 32 CT states per molecule.

could say that the reason why qV_{oc} is almost always 0.5–0.7 eV below E_{ct}^{exp} is because the CT state recombination lifetime is rarely higher than 10 ns since this is the timescale for dynamic interfacial reconfiguration and it is never lower than 10 ps since this would prevent the photogeneration of free carriers. Three orders of magnitude of change in CT state lifetime corresponds to a 180 mV difference in V_{oc} at 300 K since the CT state lifetime affects the voltage logarithmically. Because the exciton diffusion length in organic photovoltaic materials is typically <30 nm, the community has not been able to explore orders of magnitude differences in donor/acceptor mixing ratios. It has been observed, however, that in dilute blends, where you can measure the interfacial area by the strength of the CT state absorption, V_{oc} does depend logarithmically on interfacial area in agreement with our expression.^[66]

10. Opportunities for Improving V_{oc}

In addition to explaining why the open-circuit voltage of organic solar cells is low even though their internal quantum efficiencies can be quite high, this study also provides a framework in which to identify and rank opportunities to raise V_{oc} . Table 2 summarizes the potential gains in open-circuit voltage that could be achieved by improving each of the terms that appears in our expression for V_{oc} . Since many of the parameters appear in a logarithm, they would need to be changed by orders of magnitude to significantly enhance the open-circuit voltage.

Table 2. The potential increases that could be obtained from improvements to each of the material parameters that affects V_{oc} .

Parameter improvement strategy	V_{oc} increase
Reduce volume fraction (f) of mixed phase from 50% to 1%	100 meV
Increase CT state lifetime (τ_{ct}) from 100 ps to 10 ns	120 meV
Decrease interfacial disorder (σ_{ct}) from 100 to 50 meV	150 meV
Decrease CT state binding energy (E_b) from 200 to 50 meV	150 meV
Decrease number of CT states per interface from 30 to 3	60 meV

However, both the degree of interfacial disorder and the CT state binding energy are outside of the logarithm, implying that the largest voltage gains are likely to come from reductions in those two parameters.

A promising route to improving the open-circuit voltage of organic solar cells could be engineering the donor and acceptor molecules to dock in preferred orientations in order to reduce conformational disorder at the interface.^[67] As an example of the effect of conformational disorder on V_{oc} we compared the interfacial disorder in regiorandom and regioregular P3HT blended with PCBM. The regiorandom blend was found to have 104 meV of interfacial disorder compared with 75 meV in the regioregular blend (see Figure 5). According to our model, this slight reduction in interfacial disorder contributes ≈ 100 mV to the open-circuit voltage of the regioregular blend. In this case however, the increase in V_{oc} due to reduced disorder is overshadowed by the fact that the center of the CT state distribution for the regioregular blend is 0.4 eV lower in energy than the regiorandom blend due to the well-known differences in polymer Ionization Potential in the two systems, so the overall open-circuit voltage is lower for regioregular P3HT than for regiorandom P3HT.^[68] The measured values of 63–104 meV of interfacial energetic disorder imply that 77–210 mV of open-circuit voltage are lost to this effect in the five systems studied.

Further increases in V_{oc} could come from reductions in the CT state binding energy either by designing molecules with increased amounts of wavefunction delocalization or from raising the bulk dielectric constant of the active layer. While it may seem that large increases in dielectric constant would be needed for significant improvements in V_{oc} , Chen et al. have suggested that even a dielectric constant near 5 could be enough to largely eliminate the CT state binding energy, presumably because as the dielectric constant increases the CT states also become more delocalized, which further reduces their binding energy.^[14]

Another way to improve the open-circuit voltage would be to increase the CT state lifetime. The lifetime is known to be dominated by nonradiative transitions with an electroluminescence quantum efficiency typically worse than 10^{-6} .^[11]

This means that six orders of magnitude of improvements in CT state lifetime are possible but there is currently not a clear understanding of precisely what mechanism is leading to such fast nonradiative recombination. Future studies focused on this point could help recover some of the >360 mV of V_{oc} currently lost to this effect. We speculate that perhaps the dynamic nature of the donor/acceptor interface plays a large role in allowing CT states to find configurations that lead to fast nonradiative recombination. In that case, rigidly locking the donor/acceptor conformation could be key to increasing the radiative quantum efficiency and hence V_{oc} .

11. Conclusions

We have shown that the available experimental evidence strongly points toward a model of recombination in organic solar cells where free carriers are in equilibrium with CT states. This description simplifies understanding the recombination process and enabled us to directly link the low open-circuit voltage of organic solar cells to a combination of their high degree of mixing, short CT state lifetimes, large amounts of interfacial energetic disorder, and low dielectric constants leading to high CT state binding energies. We quantify the impact of each of these parameters and physically explain both the dependence of qV_{oc} on E_{ct}^{exp} and the generally observed 0.5–0.7 eV difference between them. Our work shows that there is significant practical potential for improving V_{oc} , provided we target the right parameters. For example, reducing interfacial energetic disorder and the CT state binding energy could raise V_{oc} by hundreds of mV without requiring any change to the CT state lifetime or degree of mixing. The picture of V_{oc} that emerges is one of a quantity that is limited mainly by the microscopic details of the interface between donor and acceptor molecules. By optimizing this interface, the OPV community has the opportunity to significantly enhance the efficiency of organic solar cells through increases in open-circuit voltage.

12. Experimental Section

Sample Preparation: Substrates used for FTPS (Fourier transform photocurrent spectroscopy) samples were ITO-coated (indium tin oxide) glass (Xinyan Technologies, Ltd.). Substrates were immersed in a detergent solution of 1:9 extran:deionized water solution then scrubbed with a brush. Samples were then sonicated in the detergent solution, rinsed with deionized water, sonicated in acetone, sonicated in isopropanol, and blown dry with nitrogen. Substrates were stored in an oven held at 115 °C. Immediately before depositing films onto substrates, substrates were exposed to a UV–ozone plasma for 15 min. PC60BM was purchased from Solenne BV. RRA-P3HT was obtained from Reike. A solution of 1:4 wt:wt RRA-P3HT:PC60BM was prepared in chloroform at a polymer concentration of 4 mg mL⁻¹, and was heated and stirred at 70 °C overnight. The RRA-P3HT:PC60BM film was deposited in a nitrogen filled glovebox (H₂O and O₂ levels typically < 10 ppm) onto prepared substrates via spin-coating at 1000 rpm for 45 s with a ramp speed of 500 rpm s⁻¹. Top electrodes consisting of 7 nm of calcium and then 250 nm of aluminum were deposited via thermal evaporation ($\approx 1 \times 10^{-7}$ Torr).

FTPS Measurements: Temperature-dependent FTPS measurements of the 1:4 RRA-P3HT:PCBM sample were performed using a Nicolet iS50R FT-IR spectrometer, with signal amplified using a Stanford Research

Systems Model SR570 low-noise current pre-amplifier. Samples were mounted on the cold finger of a Janis Research Company ST-100H cryostat. Thermal paste was used to maintain good thermal contact between the cold finger and the sample. Sample temperature was controlled using a LakeShore 331 Temperature Controller. The sample was measured at several temperatures from 82 to 300 K. Before each measurement, the sample temperature was set to the desired value with the temperature controller and then allowed to stabilize until less than 0.05 K variation in temperature was observed. The photocurrent spectrum was then recorded with no band pass filter, and with two bandpass filters which blocked all transmission of light with wavenumber larger than $\approx 13\,800$ and $12\,088$ cm⁻¹, respectively. The three resulting spectra were stitched together, prioritizing the spectra generated with the lowest wavenumber bandpass filter, to create a photocurrent spectrum for the sample.

Charge Transfer Parameter Determination: Values of E_{ct}^{exp} and λ^{exp} were determined for each temperature independently. To determine E_{ct}^{exp} and λ^{exp} , the sub-bandgap absorption was fit to Marcus theory absorption expression shown in the Supporting Information using a linear least squares fitting procedure. Under the assumption that Marcus theory is a good description of the CT absorption, the fit was restricted to the portion of the sub-bandgap absorption whose natural log had a linear first derivative (i.e., $(d(\ln(E^{\alpha}\alpha(E)))/dE$ is linear).

Supporting Information

Supporting Information is available from the Wiley Online Library or from the author.

Acknowledgements

This work was supported by the Department of the Navy, Office of Naval Research Award No. N00014-14-1-0580. T.B. was supported by a National Science Foundation Graduate Research Fellowship under Grant No. DGE-1147470. Additional support was provided by Stanford University via a Stanford Graduate Fellowship.

Received: January 16, 2015

Revised: February 19, 2015

Published online:

- [1] D. A. R. Barkhouse, O. Gunawan, T. Gokmen, T. K. Todorov, D. B. Mitzi, *Prog. Photovolt. Res. Appl.* **2012**, *20*, 6.
- [2] J. A. Bartelt, Z. M. Beiley, E. T. Hoke, W. R. Mateker, J. D. Douglas, B. A. Collins, J. R. Tumbleston, K. R. Graham, A. Amassian, H. Ade, J. M. J. Fréchet, M. F. Toney, M. D. McGehee, *Adv. Energy Mater.* **2013**, *3*, 364.
- [3] Z. He, C. Zhong, S. Su, M. Xu, H. Wu, Y. Cao, *Nat. Photonics* **2012**, *6*, 593.
- [4] K. R. Graham, P. Erwin, D. Nordlund, K. Vandewal, R. Li, G. O. N. Ndjawa, E. T. Hoke, A. Salleo, M. E. Thompson, M. D. McGehee, A. Amassian, *Adv. Mater.* **2013**, *25*, 6076.
- [5] C. M. Proctor, J. A. Love, T. Q. Nguyen, *Adv. Mater.* **2014**, *26*, 5957.
- [6] C. Gu, Y. Chen, Z. Zhang, S. Xue, S. Sun, C. Zhong, H. Zhang, Y. Lv, F. Li, F. Huang, Y. Ma, *Adv. Energy Mater.* **2014**, *4*, 1301771.
- [7] C. Deibel, V. Dyakonov, *Rep. Prog. Phys.* **2010**, *73*, 68.
- [8] B. Kippelen, J.-L. Brédas, *Energy Environ. Sci.* **2009**, *2*, 251.
- [9] T. M. Clarke, J. R. Durrant, *Chem. Rev.* **2010**, *110*, 6736.
- [10] E. T. Hoke, K. Vandewal, J. A. Bartelt, W. R. Mateker, J. D. Douglas, R. Noriega, K. R. Graham, J. M. J. Fréchet, A. Salleo, M. D. McGehee, *Adv. Energy Mater.* **2013**, *3*, 220.

- [11] K. Vandewal, K. Tvingstedt, A. Gadisa, O. Inganäs, J. V. Manca, *Phys. Rev. B* **2010**, *81*, 1.
- [12] K. Vandewal, K. Tvingstedt, A. Gadisa, O. Inganäs, J. V. Manca, *Nat. Mater.* **2009**, *8*, 904.
- [13] N. Cho, C. W. Schlenker, K. M. Knesting, P. Koelsch, H. L. Yip, D. S. Ginger, A. K. Y. Jen, *Adv. Energy Mater.* **2014**, *4*, 1301857.
- [14] S. Chen, S. W. Tsang, T. H. Lai, J. R. Reynolds, F. So, *Adv. Mater.* **2014**, *26*, 6125.
- [15] S. Sweetnam, K. R. Graham, G. O. N. Ndjawa, T. Heumueller, J. A. Bartelt, T. M. Burke, W. Li, W. You, A. Amassian, M. D. McGehee, *J. Am. Chem. Soc.* **2014**, *40*, 14078.
- [16] T. M. Burke, M. D. McGehee, *Adv. Mater.* **2014**, *26*, 1923.
- [17] M. M. Mandoc, L. J. A. Koster, P. W. M. Blom, *Appl. Phys. Lett.* **2007**, *90*, 133504.
- [18] J. C. Blakesley, D. Neher, *Phys. Rev. B* **2011**, *84*, 075210.
- [19] F. C. Jamieson, E. B. Domingo, T. McCarthy-Ward, M. Heeney, N. Stingelin, J. R. Durrant, *Chem. Sci.* **2012**, *3*, 485.
- [20] D. A. Vithanage, A. Devižis, V. Abramavičius, Y. Infahsaeng, D. Abramavičius, R. C. I. MacKenzie, P. E. Keivanidis, A. Yartsev, D. Hertel, J. Nelson, V. Sundström, V. Gulbinas, *Nat. Commun.* **2013**, *4*, 2334.
- [21] S. Gélinas, A. Rao, A. Kumar, S. L. Smith, A. W. Chin, J. Clark, T. S. van der Poll, G. C. Bazan, R. H. Friend, *Science* **2014**, *343*, 512.
- [22] G. Lakhwani, A. Rao, R. H. Friend, *Annu. Rev. Phys. Chem.* **2014**, *65*, 557.
- [23] R. A. J. Janssen, J. Nelson, *Adv. Mater.* **2013**, *25*, 1847.
- [24] G.-J. A. H. Wetzelaer, M. Kuik, P. W. M. Blom, *Adv. Energy Mater.* **2012**, *2*, 1232.
- [25] S. R. Cowan, A. Roy, A. J. Heeger, *Phys. Rev. B* **2010**, *82*, 245207.
- [26] C. Groves, R. G. E. Kimber, A. B. Walker, *J. Chem. Phys.* **2010**, *133*, 144110.
- [27] C. Groves, R. A. Marsh, N. C. Greenham, *J. Chem. Phys.* **2008**, *129*, 114903.
- [28] P. C. Y. Chow, S. Gélinas, A. Rao, R. H. Friend, *J. Am. Chem. Soc.* **2014**, *136*, 3424.
- [29] P. W. M. Blom, M. J. M. de Jong, S. Breedijk, *Appl. Phys. Lett.* **1997**, *71*, 930.
- [30] G. A. H. Wetzelaer, M. Kuik, H. T. Nicolai, P. W. M. Blom, *Phys. Rev. B* **2011**, *83*, 165204.
- [31] J. J. M. van der Holst, F. W. A. van Oost, R. Coehoorn, P. A. Bobbert, *Phys. Rev. B* **2009**, *80*, 235202.
- [32] C. Groves, N. Greenham, *Phys. Rev. B* **2008**, *78*, 155205.
- [33] C. M. Proctor, M. Kuik, T.-Q. Nguyen, *Prog. Polym. Sci.* **2013**, *38*, 1941.
- [34] J. Kniepert, I. Lange, N. J. Van Der Kaap, L. J. A. Koster, D. Neher, *Adv. Energy Mater.* **2014**, *4*, 1301401.
- [35] B. Ray, M. A. Alam, *IEEE J. Photovolt.* **2012**, *2*, 1.
- [36] S. Y. Leblebici, T. L. Chen, P. Olalde-Velasco, W. Yang, B. Ma, *ACS Appl. Mater. Interfaces* **2013**, *5*, 10105.
- [37] N. Cho, C. W. Schlenker, K. M. Knesting, P. Koelsch, H. L. Yip, D. S. Ginger, A. K. Y. Jen, *Adv. Energy Mater.* **2014**, *4*, 1301857.
- [38] K. Vandewal, A. Gadisa, W. D. Oosterbaan, S. Bertho, F. Banishoeib, I. Van Severen, L. Lutsen, T. J. Cleij, D. Vanderzande, J. V. Manca, *Adv. Funct. Mater.* **2008**, *18*, 2064.
- [39] U. Hörmann, J. Kraus, M. Gruber, C. Schuhmair, T. Linderl, S. Grob, S. Kapfinger, K. Klein, M. Stutzman, H. Krenner, W. Brütting, *Phys. Rev. B* **2013**, *88*, 235307.
- [40] K. Vandewal, S. Albrecht, E. T. Hoke, K. R. Graham, J. Widmer, J. D. Douglas, M. Schubert, W. R. Mateker, J. T. Bloking, G. F. Burkhard, A. Sellinger, J. M. J. Fréchet, A. Amassian, M. K. Riede, M. D. McGehee, D. Neher, A. Salleo, *Nat. Mater.* **2014**, *13*, 63.
- [41] M. L. Jones, R. Dyer, N. Clarke, C. Groves, *Phys. Chem. Chem. Phys.* **2014**, *16*, 20310.
- [42] C. Groves, *Energy Environ. Sci.* **2013**, *6*, 1546.
- [43] I. A. Howard, F. Etzold, F. Laquai, M. Kemerink, *Adv. Energy Mater.* **2014**, *4*, 1301743.
- [44] V. Abramavičius, D. Amarasinghe Vithanage, A. Devižis, Y. Infahsaeng, A. Bruno, S. Foster, P. E. Keivanidis, D. Abramavičius, J. Nelson, A. Yartsev, V. Sundström, V. Gulbinas, *Phys. Chem. Chem. Phys.* **2014**, *16*, 2686.
- [45] M. Hilczler, M. Tachiya, *J. Phys. Chem. C* **2010**, *114*, 6808.
- [46] P. Wurfel, *J. Phys. C: Solid State Phys.* **1982**, *15*, 3967.
- [47] S. T. Hoffmann, H. Bässler, A. Köhler, *J. Phys. Chem. B* **2010**, *114*, 17037.
- [48] L. Kador, *J. Chem. Phys.* **1991**, *95*, 5574.
- [49] J. C. Blakesley, N. C. Greenham, *J. Appl. Phys.* **2009**, *106*, 034507.
- [50] K. Vandewal, K. Tvingstedt, O. Inganäs, *Quantum Efficiency in Complex Systems, Part II*, Academic Press, San Diego, California **2011**, pp. 261.
- [51] B. Rand, D. Burk, S. Forrest, *Phys. Rev. B* **2007**, *75*, 115327.
- [52] N. C. Giebink, G. P. Wiederrecht, M. R. Wasielewski, S. R. Forrest, *Phys. Rev. B* **2010**, *82*, 155305.
- [53] C. G. Shuttle, A. Maurano, R. Hamilton, B. O'Regan, J. C. de Mello, J. R. Durrant, *Appl. Phys. Lett.* **2008**, *93*, 183501.
- [54] D. Credgington, J. R. Durrant, *J. Phys. Chem. Lett.* **2012**, *3*, 1465.
- [55] K. Vandewal, L. Goris, I. Haelderms, M. Nesládek, K. Haenen, P. Wagner, J. V. Manca, *Thin Solid Films* **2008**, *516*, 7135.
- [56] L. Goris, A. Poruba, L. Hod'Ákova, M. Vaněček, K. Haenen, M. Nesládek, P. Wagner, D. Vanderzande, L. De Schepper, J. V. Manca, *Appl. Phys. Lett.* **2006**, *88*, 1.
- [57] K. Tvingstedt, K. Vandewal, A. Gadisa, *J. Am. Chem. Soc.* **2009**, *131*, 11819.
- [58] J. H. Choi, K.-I. Son, T. Kim, K. Kim, K. Ohkubo, S. Fukuzumi, *J. Mater. Chem.* **2010**, *20*, 475.
- [59] D. Veldman, O. Ipek, S. C. J. Meskers, J. Sweelssen, M. M. Koetse, S. C. Veenstra, J. M. Kroon, S. S. van Bavel, J. Loos, R. A. J. Janssen, *J. Am. Chem. Soc.* **2008**, *130*, 7721.
- [60] A. A. Bakulin, A. Rao, V. G. Pavelyev, P. H. M. van Loosdrecht, M. S. Pshenichnikov, D. Niedzialek, J. Cornil, D. Beljonne, R. H. Friend, *Science* **2012**, *335*, 1340.
- [61] T. Liu, A. Troisi, *J. Phys. Chem. C* **2011**, *115*, 2406.
- [62] T. Liu, D. L. Cheung, A. Troisi, *Phys. Chem. Chem. Phys.* **2011**, *13*, 21461.
- [63] H. Ma, A. Troisi, *Adv. Mater.* **2014**, *26*, 6163.
- [64] B. M. Savoie, A. Rao, A. A. Bakulin, S. Gélinas, B. Movaghar, R. H. Friend, T. J. Marks, M. A. Ratner, *J. Am. Chem. Soc.* **2014**, *136*, 2876.
- [65] R. A. Street, D. Davies, P. P. Khlyabich, B. Burkhart, B. C. Thompson, *J. Am. Chem. Soc.* **2013**, *135*, 986.
- [66] K. Vandewal, J. Widmer, T. Heumueller, C. J. Brabec, M. D. McGehee, K. Leo, M. Riede, A. Salleo, *Adv. Mater.* **2014**, *26*, 3839.
- [67] K. R. Graham, C. Cabanetos, J. P. Jahnke, M. N. Idso, A. El Labban, G. O. Ngongang Ndjawa, T. Heumueller, K. Vandewal, A. Salleo, B. F. Chmelka, A. Amassian, P. M. Beaujuge, M. D. McGehee, *J. Am. Chem. Soc.* **2014**, *136*, 9608.
- [68] W. C. Tsoi, S. J. Spencer, L. Yang, A. M. Ballantyne, P. G. Nicholson, A. Turnbull, A. G. Shard, C. E. Murphy, D. D. C. Bradley, J. Nelson, J. S. Kim, *Macromolecules* **2011**, *44*, 2944.